Mixing Performance of Arrow-Shaped Micro-Devices

Chiara Galletti*, Elisabetta Brunazzi, Lorenzo Siconolfi, Deborah Spaltro, Roberto Mauri

Dipartimento di Ingegneria Civile e Industriale, Università di Pisa, Largo Lucio Lazzarino 2, 56122 Pisa, Italy.
chiara.galletti@unipi.it

The process of liquid laminar mixing in arrow-shaped micro-devices is studied by direct numerical simulations. Two different CFD codes, i.e. Fluent (based on finite volume method) and Nek5000 (based on spectral element method) have been used to investigate the flow and concentration fields. Unexpectedly we observe that within the engulfment regime, the degree of mixing first increases and then diminishes as the inlet flow rate is increased. Such reduction in the degree of mixing, not observed in T-shaped mixers, can be imputed to the presence of a strong vortical structure at the center of the mixing channel. This result is important for control operations, as it shows that on one hand arrow type mixers are characterized by higher degree of mixing with respect to T-shaped mixers, but on the other hand they present a narrower range of optimal conditions.

1. Introduction

Continuous flow micro-reactors are receiving an increasing attention in the fine chemical and pharmaceutical industries, as they enhance heat and mass transfer operations due to their high surface-to-volume ratio. Moreover, the scale-up procedure that is needed in conventional batch operations is avoided here, as it is replaced by a simple numbering-up of reactors (Plouffe et al., 2016).

The main difficulty of micro-mixing is that the flow is laminar, so transport phenomena are relatively slow. Therefore, many mixer geometries have been investigated in order to enhance mixing by splitting and recombination of fluid streamlines (Roudgar et al., 2012). Among the most studied micromixers, there are T- and Y-devices, in which the inlet channels join the mixing channels with T and Y geometries. These reactors are also suitable for fundamental studies, as they are often used as junction elements in more complex networks (Galletti et al., 2015a).

In the case of T-mixers, at low Reynolds number, Re, the flow streams remain segregated, as mixing is induced by molecular diffusion only. Then, increasing Re, the flow structure shows a pair of counter-rotating vortices, with double mirror symmetry, corresponding, again, to a low degree of mixing. Further increasing the flow rate, a symmetry breaking occurs, leading to a pair of co-rotating vortical structures, with central point symmetry. This, so called, engulfment regime is very interesting, because of the rapid increase of the degree of mixing at its onset (Galletti et al., 2015b). Further increasing Re, the flow becomes first unsteady and time-periodic, and eventually chaotic (Andreussi et al., 2015). Fani et al. (2013) showed through stability analysis that the engulfment regime is driven by the tilting of the flow structures near the top of the mixer. Moreover, they performed a sensitivity analysis to determine the regions within the micromixer where any small perturbation produces large effects. Based on these results, Siconolfi et al. (2016) suggested to use an arrow-type micromixer, as the arrow junction is able to disturb such region and hence trig the symmetry breaking. Indeed, the aforementioned authors showed that the Re at which the engulfment regime occurs in arrow-type mixers is anticipated with respect to T-mixers.

The present work is aimed at extending the investigation by Siconolfi et al. by analysing arrow-type mixers characterized by different aspect ratios and determining their efficiency in terms of the dependence of the degree of mixing on the Reynolds number.

2. Flow configuration

In the present configuration, two identical liquid streams converge onto an arrow-type junction with α = 20°, as shown in Figure 1, along with the reference system. Such α = 20° was found to be very effective for anticipating the Reynolds number at which engulfment occurs by Siconolfi et al. (2016). The inlet channels are equal with depth H, width Wi and length Li. The mixing channel has a width, which is twice that of the inlet channels (i.e., W = 2Wi) and a length L.

Two different cases were investigated corresponding to Wi=H (i.e., square cross section of the inlet channel) and Wi=3/4H. In all cases the length of the inlet channels was chosen to include the confluence region, i.e. Li = 2.25d. Here d is the hydraulic diameter of the mixing (outlet) channel. The length of the mixing channel, L, was long enough to completely describe the complex vortical structures and avoid any channel-length effect on the predictions (Andreussi et al., 2015).
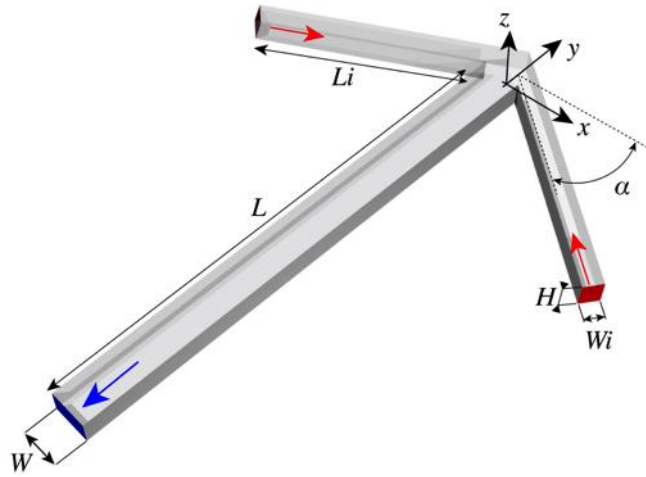

Figure 1: Sketch of the Y-shaped mixer.

3. Governing equations and numerical model

When a small quantity of dye is added to one of the inlet fluids, the governing equations at steady state are:

$$\nabla \cdot \mathbf{u} = 0; \quad \mathbf{u} \cdot \nabla \mathbf{u} + \nabla P = \mathrm{Re}^{-1} \nabla^2 \mathbf{u}; \quad \mathbf{u} \cdot \nabla f = \mathrm{Pe}^{-1} \nabla^2 f \qquad (1)$$

Here ϕ is the normalized dye mass fraction (i.e., $0<\phi<1$), $\mathbf{u}$ is the dye non-dimensional velocity (which coincides with the fluid velocity, due to the dye diluteness), whereas P is the reduced pressure. All terms are non-dimensionalised using the mixing channel hydraulic diameter, d, and the mean bulk velocity, U (which is the same in the mixing and in the inlet channels). Re is the Reynolds number in the mixing channel, i.e. Re=Ud/v, and Pe is the Peclet number, Pe = Ud/D, with v and D denoting the kinematic viscosity and the molecular diffusivity, respectively.

These equations are solved with boundary conditions consisting of no-slip velocity and no-mass-flux at the channel walls, a constant ambient pressure at the exit, while at the entrance a flow profile corresponding to fully developed flow conditions in a square conduit (Happel and Brenner, 1965) was imposed through a bespoke subroutine as described in Galletti et al. (2012). The two fluids are fed with the same flow rate.

The efficiency of the mixing process is described using the degree of mixing, δ_m, defined in terms of bulk averages, as shown in Orsi et al. (2013a),

$$\delta_m = 1 - \frac{S_b(y)}{S_{max}}; \qquad S_b^2(y) = \frac{1}{N\bar{u}} \sum_{i=1}^{N} \left(f_i - \bar{f}_b\right)^2 u_i; \qquad \bar{\phi}_b = \frac{\sum \phi_i u_i}{N\bar{u}} = \frac{1}{2};$$

$$\sigma_{max} = \sqrt{\bar{\phi}_b\left(1-\bar{\phi}_b\right)} = \tfrac{1}{2}. \qquad (2)$$

Here, all quantities are defined within a cross section at a distance y from the confluence, N are the grid points in the cross section, σ_b is the standard deviation of the local mass fraction ϕ from its constant mean bulk value, $\bar{f}_b$, and σ_{max} denotes the maximum value of σ_b, that is achieved when the two streams are completely segregated.

Finally, the vortical structures in a cross section are represented through the λ_2-criterion (Jeong & Hussain, 1995), which is based on the concept that a vortex is associated with a local pressure minimum. Accordingly, a vortex is defined as a connected fluid region where the second eigenvalue of the symmetric tensor $S_2+\Omega_2$ is negative, i.e. $\lambda_2<0$, with S and Ω indicating the strain rate and vorticity tensors, respectively, i.e. $\nabla\mathbf{u} = S+W$. Simulations were performed using two different CFD codes.

The Wi=H case (i.e. square inlet) was investigated with the commercial finite volume code ANSYS Fluent® v. 15, using a grid of cubic elements with H/20 edge, leading to 20 x 40 elements in each cross section of the mixing channel and a total of 384k elements. Such grid resulted from a grid independency study, performed using from 300k to 800k elements. Steady state simulations were carried out with second order discretization scheme and SIMPLE algorithm for pressure-velocity coupling. Simulations were typically considered converging when the normalized residuals for velocities were stationary with iterations and fell below 10^{-12}. Such small residuals were specifically required to ensure converged solutions near the engulfment (Orsi et al., 2013b, Galletti et al., 2012). The steadiness of the solution with iterations was also assessed by checking the velocity and concentration field in the outlet section of the mixing channels at different iterations.

The Wi = 3/4H case was studied with the massively parallel spectral-element code Nek5000 (https://nek5000.mcs.anl.gov). The spatial discretization of the domain consists of a 16000 hexahedral elements; the unknown variables are spanned by N^{th}-order Lagrange polynomial interpolants, where N = 8 for velocity and the passive scalar and N=6 for pressure. Concerning the time discretization, a third order backward differential formula is employed for the time derivatives and the time step is chosen to satisfy the condition Courant number less than 0.5. This setup resulted in 6×10^6 degrees of freedom (dofs) for each velocity component (and the passive scalar) and 3.5×10^6 dofs for the pressure.

4. Results

The flow structures identified through the λ_2-criterion for the square inlet case (i.e. Wi=H) using the Fluent code are shown in Figure 2 at different Reynolds numbers. For Re = 120, the flow shows a four-leg pattern and a clear double mirror symmetry, with two counter rotating vortex pairs (vortex regime, see Figure 2a). As the flow rate is increased, we observe a symmetry breaking instability, which leads to an asymmetric regime, characterized by a two-leg pattern (engulfment regime, see Figure 2b). Such symmetry breaking occurs at Re = 133 and hence it is anticipated with respect to the T-shaped mixers for which it occurs at Re = 138 (Galletti et al., 2015b).
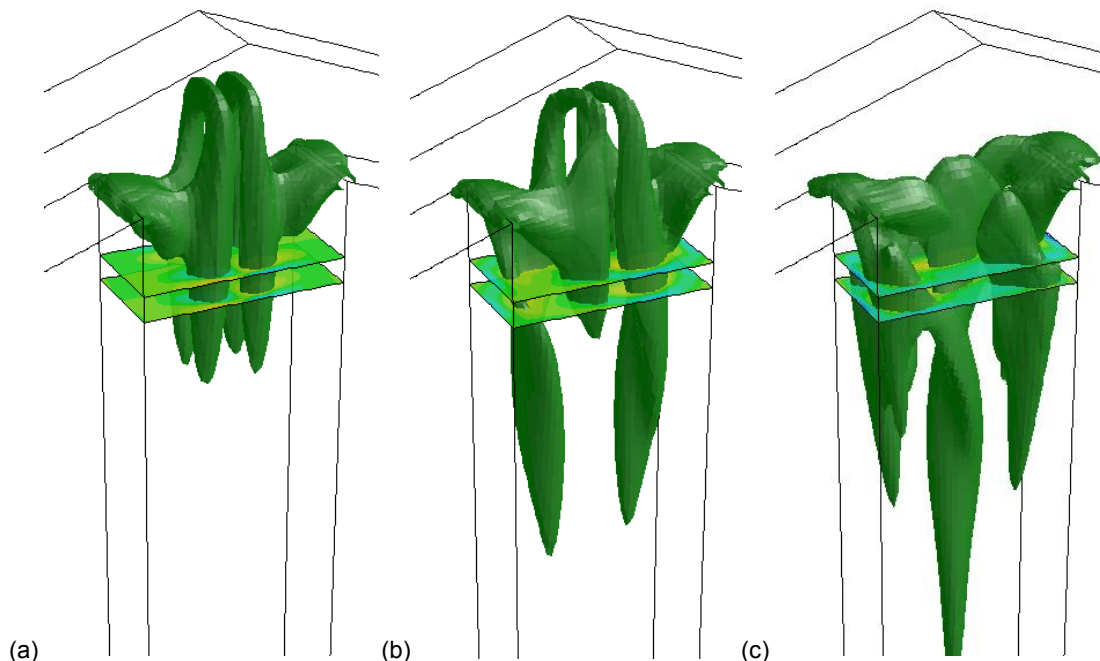

Figure 2: Vortical structures as identified through the λ_2-criterion for different Reynolds numbers, i.e. Re = (a) 120; (b) 133; (c)170. Wi=H, Fluent code.

Further increasing Re, we observe unexpectedly the presence of a strong vortical structure at the centre of the mixing channel resulting from the merging of two vortical structures in the upper region of the mixer (Re = 170, see Figure 2c).

The Nek5000 simulations confirmed similar behaviour also for the Wi=3/4H case, as can be observed by the vortical structures shown in Figure 3. Logically the Reynolds numbers are different as the aspect ratio of the inlet channels is different (Andreussi et al., 2015). The Re = 100 case clearly indicates a vortex regime, whereas Re = 130 shows an engulfment regime. Please note that the tilt angle of the vortical structures at the top of the mixer can be either positive or negative due to the symmetry of the mixer, that means that the flow stream from the right can move either to the front or to the back by chance. In particular we can notice that the engulfment is predicted with positive tilt angle by Fluent (Figure 2b) and negative tilt angle by Nek5000 (Figure 3b), but this occurs by chance.
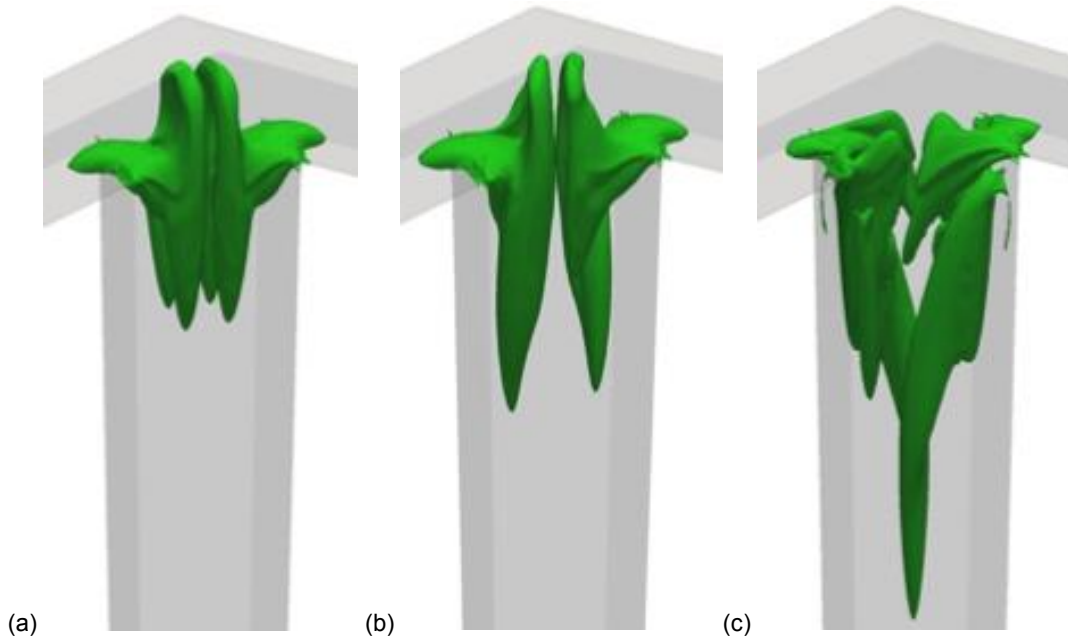

(a)   (b)   (c)

Figure 3: Vortical structures as identified through the λ_2-criterion for different Reynolds numbers, i.e. Re = (a) 100; (b) 130; (c)170. Wi=3/4H, Nek5000 code.

The y vorticity in the mixing channel cross-section at y = -3d clearly shows the double mirror symmetry with a double pair of counter-rotating vortices in the vortex regime (Figure 4a), a symmetry breaking and point-wise symmetry in the engulfment regime (Figure 4b) and then the merging of the vortical structures at the centre of the channel by further increasing Re (Figure 4c). This latter behaviour is not encountered in T-shaped mixers.
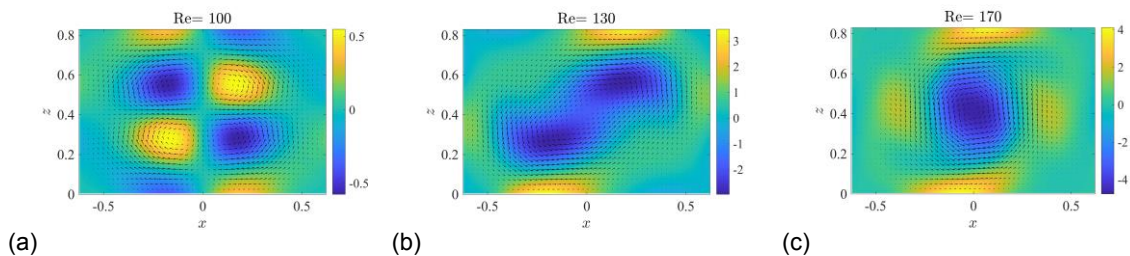

(a)   (b)   (c)

Figure 4: contours of y vorticity in the mixing channel cross section at y = -3d for different Reynolds numbers, i.e. Re = (a) 100; (b) 130; (c)170. Wi=3/4H, Nek5000 code.
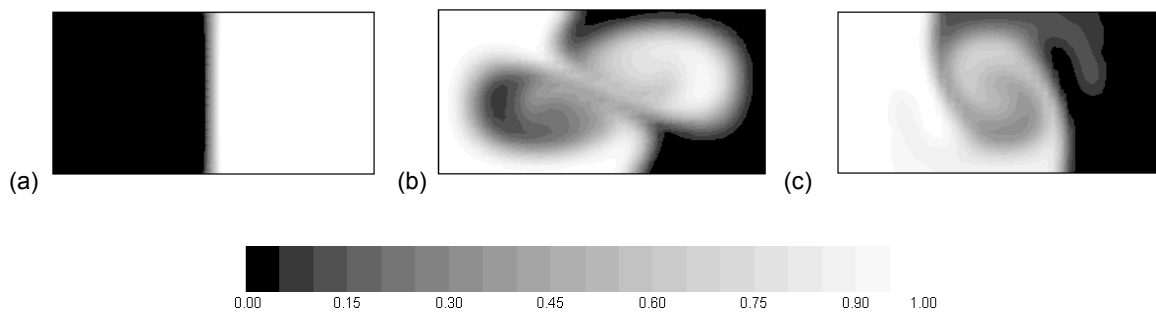
Figure 5: Distribution of the scalar concentration at the mixing channel outlet for different Reynolds numbers, i.e. Re = (a) 120; (b) 133; (c)170. Wi=H, Fluent code.

Figure 5 shows the scalar concentration distribution for the square inlet case at the outlet of the mixing channel, clearly highlighting the flow stream segregation in the vortex regime and the strong mixing promoted by the engulfment (see Figure 5a and Figure 5b at Re = 120 and Re = 130, respectively). However, further increasing the Re, the presence of a vortical structure at the centre of the mixing leads to a completely different concentration pattern (see Figure 5c at Re=170) with a mixing that seems to be lower that that observed for smaller Reynolds number (i.e., Re = 133).

Figure 6 shows the degree of mixing, δ_m, as a function of Re for the square inlet case when α = 0° (i.e., a T-mixer) and α = 20° (arrow-type mixer). The T-mixer shows a steep increase of mixing corresponding to the onset of the engulfment regime and a monotonic increase up to Re = 213. Further increasing Re an unsteady time-periodic regime is observed (Andreussi et al., 2015). Instead and unexpectedly, for the arrow-type mixer we found that, by increasing Re in the engulfment regime, the degree of mixing first increases and then diminishes. Such reduction can be imputed to the formation of a high velocity region at the centre of the mixer channel. This result is important for control operations, as it shows that on one hand arrow type mixers are characterized by higher degree of mixing with respect to T-shaped mixers, but on the other hand they present a narrower range of optimal conditions.
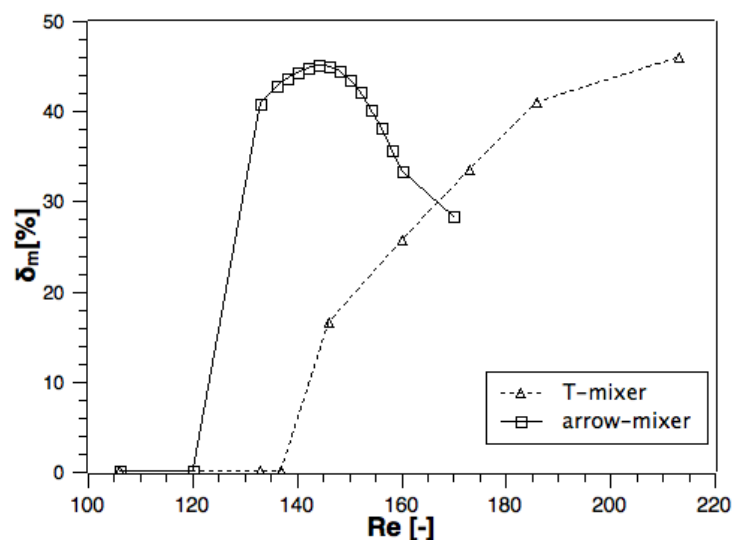

Figure 6: Degree of mixing as a function of the Reynolds number for T- and arrow-type mixers. Wi=H, Fluent code.

5. Conclusions

Two different CFD codes, i.e. Fluent (based on finite volume method) and Nek5000 (based on spectral element method), have been used to investigate the flow and concentration fields in an arrow-shaped micro-mixer.

Despite the different numerics and different arrow-type mixer aspect ratios used in the investigations, results indicated similar vortical structures, hence validating the modeling approach. In particular, at low Reynolds numbers the inlet streams remain well segregated, with the presence of a double pair of counter-rotating vortical structures in the mixing channel. This regime is very similar to that observed in T-shaped mixers. With further increasing Re, a symmetry breaking occurs leading to the engulfment regime, triggered by the tilting of the vortical structures at the top of the vessel, with a mechanism similar to that encountered in T-mixers. Such regime provides a sharp increase of the degree of mixing. However with further increasing the Reynolds number, an unexpected reduction of the degree of mixing is observed. Such reduction, not observed in T-mixers, is due to the presence of a strong vortical structure at the center of the mixing channel. Hence, although an arrow-shaped geometry is able to anticipate the Reynolds number promoting the engulfment with respect to T-mixers, it provides a narrower range of optimal operation conditions.

Reference

Andreussi T., Galletti C., Mauri R., Camarri S., Salvetti M.V., 2015, Flow regimes in T-shaped micro-mixers, Computers and Chemical Engineering, 76, 150-159.

Fani A., Camarri S., Salvetti M.V., 2013, Investigation of the steady engulfment regime in a three-dimensional T-mixer, Physics of Fluids 25 (6), art. no. 064102.

Galletti C., Arcolini G., Brunazzi E., Mauri R., 2015a, Mixing of binary fluids with composition-dependent viscosity in a T-shaped micro-device, Chemical Engineering Science, 123, 300-310.

Galletti C., Brunazzi E., Mauri R., 2015b, Effect of composition-dependent viscosity of liquids on the performance of micro-mixers, Chemical Engineering Transactions, 43, 1645-1650, DOI: 10.3303/CET1543275.

Galletti C., Roudgar M., Brunazzi E., Mauri R., 2012, Effect of inlet conditions on the engulfment pattern in a T-shaped micro-mixer, Chemical Engineering Journal, 185-186, 300-313.

Happel J., Brenner H., 1965, Low Reynolds Number Hydrodynamics. Prentice Hall, Englewood Cliffs, NJ.

Jeong J., Hussain F., 1995, On the identification of a vortex, J. Fluid Mech. 285, 69-94.

Orsi G., Galletti C., Brunazzi E., Mauri R., 2013a, Mixing of two miscible liquids in T-shaped microdevices, Chemical Engineering Transactions, 32, 1471-1476, DOI: 10.3303/CET1332246.

Orsi G., Rougar M., Brunazzi E., Galletti C., Mauri R., 2013b, Water-ethanol mixing in T-shaped microdevices, Chemical Engineering Science, 95, 174-183.

Plouffe P., Bittel Mi., Sieber J., Roberge D. M., Macchi A., 2016, On the scale-up of micro-reactors for liquid–liquid reactions, Chemical Engineering Science, 143, 216-225.

Roudgar M., Brunazzi E., Galletti C., Mauri R., 2012, Numerical study of split T-micromixers, Chemical Engineering and Technology, 35 (7), 1291-1299.

Siconolfi L, Fani A., Camarri S., Salvetti M.V., 2016, Effect of geometry modifications on the engulfment in micromixers: numerical simulations and stability analysis, European Journal of Mechanics - B/Fluids 55, 360-366.